

# Coordination of leaf and stem water transport properties in tropical forest trees

Frederick C. Meinzer · David R. Woodruff · Jean-Christophe Domec ·  
Guillermo Goldstein · Paula I. Campanello · M. Genoveva Gatti ·  
Randol Villalobos-Vega

Received: 2 August 2007 / Accepted: 11 January 2008 / Published online: 6 February 2008  
© Springer-Verlag 2008

**Abstract** Stomatal regulation of transpiration constrains leaf water potential ( $\Psi_L$ ) within species-specific ranges that presumably avoid excessive tension and embolism in the stem xylem upstream. However, the hydraulic resistance of leaves can be highly variable over short time scales, uncoupling tension in the xylem of leaves from that in the stems to which they are attached. We evaluated a suite of leaf and stem functional traits governing water relations in individuals of 11 lowland tropical forest tree species to determine the manner in which the traits were coordinated with stem xylem vulnerability to embolism. Stomatal regulation of  $\Psi_L$  was associated with minimum values of water potential in branches ( $\Psi_{br}$ ) whose functional significance was similar across species. Minimum values of  $\Psi_{br}$  coincided with the

bulk sapwood tissue osmotic potential at zero turgor derived from pressure–volume curves and with the transition from a linear to exponential increase in xylem embolism with increasing sapwood water deficits. Branch xylem pressure corresponding to 50% loss of hydraulic conductivity ( $P_{50}$ ) declined linearly with daily minimum  $\Psi_{br}$  in a manner that caused the difference between  $\Psi_{br}$  and  $P_{50}$  to increase from 0.4 MPa in the species with the least negative  $\Psi_{br}$  to 1.2 MPa in the species with the most negative  $\Psi_{br}$ . Both branch  $P_{50}$  and minimum  $\Psi_{br}$  increased linearly with sapwood capacitance ( $C$ ) such that the difference between  $\Psi_{br}$  and  $P_{50}$ , an estimate of the safety margin for avoiding runaway embolism, decreased with increasing sapwood  $C$ . The results implied a trade-off between maximizing water transport and minimizing the risk of xylem embolism, suggesting a prominent role for the buffering effect of  $C$  in preserving the integrity of xylem water transport. At the whole-tree level, discharge and recharge of internal  $C$  appeared to generate variations in apparent leaf-specific conductance to which stomata respond dynamically.

Communicated by Manuel Lerdau.

F. C. Meinzer (✉) · D. R. Woodruff  
USDA Forest Service, Forestry Sciences Laboratory,  
3200 SW Jefferson Way, Corvallis, OR 97331, USA  
e-mail: fmeinzer@fs.fed.us; rick.meinzer@oregonstate.edu

J.-C. Domec  
Department of Forestry and Environmental Resources,  
North Carolina State University, Raleigh, NC 27695, USA

G. Goldstein · R. Villalobos-Vega  
Department of Biology, University of Miami,  
PO Box 249118, Coral Gables, FL 33124, USA

P. I. Campanello · M. G. Gatti  
Laboratorio de Ecología Funcional,  
Departamento de Ecología, Genética y Evolución,  
Facultad de Ciencias Exactas y Naturales,  
Universidad de Buenos Aires, Ciudad Universitaria,  
Pab. II, 4 piso, Buenos Aires C1428EHA, Argentina

**Keywords** Capacitance · Stomata · Transpiration ·  
Turgor · Xylem vulnerability

## Introduction

Maintaining the integrity of the xylem hydraulic continuum running from the roots to the leaves requires that the stomata be highly responsive in coordinating transpiration with dynamic variation in the efficiency of water supply to the leaves. Otherwise, transpiration-induced increases in xylem tension may result in rapid, synergistic propagation of air embolisms leading to critical levels of potentially irreversible hydraulic failure (Tyree and Sperry 1988) and

lethal levels of leaf dehydration. For a given transpiration rate and soil water potential, the magnitude of leaf water potential ( $\Psi_L$ ) is determined by the whole-plant leaf area-specific hydraulic conductance ( $K_L$ ), which has led to broad convergence in coordination between leaf gas exchange and various measures of leaf-specific hydraulic capacity among diverse species and growth forms (Meinzer et al. 1995; Brodribb et al. 2002; Mencuccini 2003; Santiago et al. 2004). Although a number of components of plant hydraulic architecture such as xylem specific conductivity (Domec et al. 2007), hydraulic capacitance ( $C$ ) (Meinzer et al. 2003; Scholz et al. 2007) and leaf hydraulic conductance (Bucci et al. 2003; Brodribb and Holbrook 2004; Woodruff et al. 2007) show substantial variation over the course of a single day, relatively little is known about the suites of functional traits involved in facilitating the dynamic coordination between plant hydraulic capacity and stomatal control of gas exchange and leaf water status.

Stomatal regulation of transpiration constrains leaf water potential within species-specific ranges. In so-called isohydric species, minimum values of  $\Psi_L$  remain essentially constant despite variation in soil water availability and atmospheric demand, whereas anisohydric species are generally characterized by increasingly negative values of minimum  $\Psi_L$  as soil water availability declines (Turner et al. 1984; Tardieu and Simonneau 1998; Bucci et al. 2005; Fisher et al. 2006). A third type of plant  $\Psi$  regulation, isohydrodynamic, in which a constant root-to-shoot  $\Delta\Psi$  is maintained seasonally, has recently been described (Franks et al. 2007). Although species may readily be placed in one of the preceding categories, the significance of various  $\Psi_L$  set points, thresholds or ranges in the context of stomatal responses to hydraulic perturbations may not be apparent. Recent analyses favor a metabolically mediated response of stomatal guard cells to localized perturbations in epidermal water status (Franks 2004; Buckley 2005). Regardless of the stomatal control mechanisms involved, broader understanding of patterns of stomatal regulation of  $\Psi_L$  requires knowledge of the hydraulic architecture of the stems to which the leaves are attached and of the leaves themselves. For example, to determine whether stomata regulate  $\Psi_L$  to avoid excessive embolism in terminal branches, both the  $\Psi$  and the hydraulic vulnerability of the branches must be assessed. Because the hydraulic resistance of leaves is substantial (Sack and Holbrook 2006), tension in the xylem of transpiring leaves can be poorly coupled to that in the stems to which they are attached (Begg and Turner 1970; Bucci et al. 2004a). Interpretation of  $\Psi_L$  alone is further complicated by mounting evidence that leaves normally experience pronounced daily cycles of loss and recovery of their hydraulic conductance, suggesting that reversible embolism

in leaves may constitute part of an essential hydraulic signal that enables stomata to maintain stem and leaf  $\Psi$  at set points that insure the integrity of the water transport system upstream (Brodribb and Holbrook 2003; Meinzer et al. 2004; Woodruff et al. 2007).

$C$  is another component of plant hydraulic architecture involved in stomatal regulation of plant water status. Although water derived from internal  $C$  typically contributes a relatively small fraction to total daily transpiration (Kobayashi and Tanaka 2001; Phillips et al. 2003; Meinzer et al. 2004), its buffering effect on daily fluctuations in xylem tension and  $\Psi_L$  should not be underestimated. Under the transient tension and flow regimes that prevail in intact plants,  $C$  has a profound impact on the relationship between  $\Psi$  gradients and water flux, especially in large trees (Holbrook and Sinclair 1992; Meinzer et al. 2003; Perämäki et al. 2005). Quasi-steady state measurements of leaf-specific conductivity in excised stem segments do not account for this effect. To the extent that  $C$  stabilizes  $\Psi_L$ , stomata should respond to its influence as to other components of hydraulic architecture that affect apparent  $K_L$ . Intrinsic  $C$  of plant tissues varies widely (Scholz et al. 2007), and a number of traits of plant–water relations, including minimum leaf and stem  $\Psi$  (Meinzer et al. 2003; Scholz et al. 2007), maximum stomatal conductance (Stratton et al. 2000; Scholz et al. 2007), maximum sap velocity (Meinzer et al. 2006) and stem xylem vulnerability (Pratt et al. 2007) have been shown to scale with sapwood  $C$  in a species-independent manner.

Broad global convergence in a variety of plant functional traits (Reich et al. 1997; Meinzer 2003; Wright et al. 2004) implies predictable evolutionary constraints on suites of characteristics governing dynamic coordination between transpiration, plant water status and hydraulic architecture. We examined coordination among a number of traits of leaf and stem water relations, some of which were considered to be dynamic in that they were subject to daily regulation, and others that represented more stable biophysical properties of an organ or tissue. These traits were studied in individuals of 11 lowland tropical forest tree species growing in two sites at opposite ends of a moisture gradient across the Isthmus of Panama. The wetter site contained a mature primary forest and the drier site contained a secondary forest. We were particularly interested in determining the extent to which stomatal regulation of  $\Psi_L$  was coordinated with stem  $\Psi$  and xylem vulnerability to embolism because the existence of consistent species-independent relationships would imply that suites of functional traits were constrained by selective pressures in a universal manner. Based on our earlier work and that of others, we hypothesized that sapwood  $C$  and reliance on stored water would be a strong determinant of the patterns observed.

## Materials and methods

### Study sites and species

The study was conducted during the dry seasons of 2003 and 2004 from two canopy cranes operated by the Smithsonian Tropical Research Institute in the Republic of Panama. Each crane is equipped with a gondola suspended by cables from a rotating jib that allows access to about 0.8 ha of forest. One crane is located in an old-growth forest in the Parque Nacional San Lorenzo on the Caribbean side of the Isthmus of Panama where the mean annual precipitation is about 3,100 mm. The other crane is located in a seasonally dry secondary forest in the Parque Natural Metropolitano near the edge of Panama City, which receives about 1,800 mm of precipitation annually with a distinct dry season between late December and April. The dry season at Parque San Lorenzo is shorter and less intense than at Parque Metropolitano. There is no overlap among tree species between the two sites. Six individuals were selected for study at the Parque San Lorenzo site and five at the Parque Metropolitano site representing a total of 11 species (Table 1).

### Leaf water relations

The pressure–volume technique (Tyree and Hammel 1972) was used to assess bulk leaf osmotic potential at zero turgor in eight of the species. Portions of terminal branches were excised in the upper canopy and their bases immediately recut under water. The cut ends remained under water with the terminal leafy portions enclosed in a plastic bag to allow partial rehydration during transit from the canopy crane to the laboratory. Individual leaves or leafy shoots

were used for pressure–volume analyses depending on petiole length and leaf size. Pressure–volume curves were initiated by first determining the fresh weight of the sample, then measuring its water potential with a pressure chamber (PMS Instrument, Albany, Ore.).

Alternate measurements of fresh weight and  $\Psi_L$  were repeated during slow dehydration on the laboratory bench until  $\Psi_L$  approached the measuring range of the pressure chamber (–4 MPa). We tested for rehydration-induced artifacts previously reported for some woody species (Bowman and Roberts 1985; Meinzer et al. 1986; Evans et al. 1990) by comparing pressure–volume curves obtained from samples at different levels of initial hydration and found none. The transition point between the non-linear and linear portions of the curve was taken to be the bulk tissue osmotic potential at zero turgor. Values of osmotic potential reported here are means from three to five curves per species. The  $\Psi$  of upper canopy leaves was determined with a pressure chamber between 0800 and 1500 hours on five dates between 16 and 24 February 2003 and seven dates between 23 February and 19 March 2004. At each sampling time, measurements were obtained from three to five leaves of each tree.

### Stem water relations

Moisture release curves for sapwood of terminal branches of ten species were determined according to the method described in Meinzer et al. (2003). Briefly, small cylinders of sapwood were allowed to hydrate in distilled water overnight, quickly blotted to remove excess water, placed in the caps of thermocouple psychrometer chambers (83 series; JRD Merrill Specialty Equipment, Logan, Utah), weighed, and then sealed inside the rest of the chamber for determination of

**Table 1** Trunk diameter, height, percent loss of hydraulic conductivity (PLC) and relative water deficit (RWD) of terminal branches at minimum branch water potentials measured in the field ( $\Psi_{br}$ ) for the measurement trees at the two study sites

Site/species	Family	Diameter (m)	Height (m)	PLC at $\Psi_{br}$	RWD at $\Psi_{br}$
Parque Nacional San Lorenzo					
<i>Manilkara bidentata</i>	Sapotaceae	0.66	30	24	0.40
<i>Protium panamense</i>	Burseraceae	0.28	16	34	0.39
<i>Tachigalia versicolor</i>	Fabaceae	0.31	23	39	0.55
<i>Tapirira guianensis</i>	Anacardiaceae	0.70	34	27	0.41
<i>Trattinnickia aspera</i>	Burseraceae	0.37	24	29	0.32
<i>Vochysia ferruginea</i>	Vochysiaceae	0.42	26	40	0.45
Parque Natural Metropolitano					
<i>Anacardium excelsum</i>	Anacardiaceae	0.98	38	–	0.25
<i>Chrysophyllum cainito</i>	Sapotaceae	0.33	23	34	–
<i>Cordia alliodora</i>	Boraginaceae	0.34	26	–	0.29
<i>Ficus insipida</i>	Moraceae	0.65	28	24	0.41
<i>Schefflera morototoni</i>	Araliaceae	0.47	22	–	0.43

water potential isotherms. Each chamber contained three cylindrical tissue samples. The psychrometer chambers were placed in an insulated water bath and allowed to equilibrate for 2–3 h before measurements were started with a 12-channel digital psychrometer meter (85 series; JRD Merrill Specialty Equipment). Measurements were repeated at 30-min intervals until the water potential values stabilized. The chambers were opened and the samples were allowed to dehydrate for different time intervals, reweighed in the psychrometer caps, resealed inside the psychrometer chambers and allowed to equilibrate for another determination of water potential. Moisture release curves were generated by plotting sapwood water potential ( $\Psi_{sw}$ ) against relative water deficit (RWD). Data points from three to four replicate curves per species were pooled. Species-specific values of sapwood  $C$  ( $\text{kg m}^{-3} \text{Mpa}^{-1}$ ) were taken as the slopes of linear regressions fitted to the initial phase of moisture release curves plotted as the cumulative mass of water released against sapwood water potential (Meinzer et al. 2003). Weight of water per unit tissue volume at saturation ( $\text{kg m}^{-3}$ ) was calculated by multiplying the saturated/dry weight ratio of each tissue by tissue density ( $\text{kg m}^{-3}$ ) and subtracting tissue density. The cumulative weight of water released per unit tissue volume was then calculated by multiplying the tissue RWD at a given value of tissue water potential by the weight of water per unit tissue volume at saturation. Sapwood osmotic potential at zero turgor was estimated by plotting sapwood moisture release curves as pressure–volume curves then determining the transition points between the non-linear and linear portions of the curves.

Hydraulic vulnerability curves for segments of terminal branches of eight species were generated using the air injection method (Sperry and Saliendra 1994). Terminal branches 2–5 cm in diameter and greater than 35 cm in length were excised near the top of the canopy. After excision, the branches were immediately re-cut under water in the crane gondola and transported to the laboratory for measurement. In the laboratory, a 15- to 17-cm-long section of each branch (0.7–1.2 cm in diameter) was cut and both ends were smoothed with clean razor blades. The stem segments were then sealed into a double-ended pressure chamber with both ends protruding and attached via tubing to an apparatus for measuring hydraulic conductivity ( $k_h$ ). The downstream end of the segment was connected to a 1-ml graduated pipette and the proximal end of the segment was attached to tubing connected to a reservoir of filtered water (0.22  $\mu\text{m}$ ) that was pressurized at 0.15 MPa for 40 min to remove emboli and restore the segment to its maximum conductivity ( $k_{h\text{max}}$ ). The pressure was then lowered to 5.5 kPa to avoid refilling of embolized vessels during the vulnerability curve procedure and the chamber was pressurized to 0.05 MPa to prevent extrusion of water

from leaf scars during measurement of axial flow. When the flow had stabilized, the time required for the meniscus in the pipette to cross five consecutive graduation marks (0.5 ml) was recorded. Maximum conductivity was calculated as the mass flow rate through the segment divided by the pressure gradient across the segment. The chamber pressure was then raised to 0.25 or 0.5 MPa depending on the species and held constant for 3 min after which the pressure was returned to 0.05 MPa and the conductivity re-measured. This process was repeated by raising the pressure in increments of 0.25–1.0 MPa up to a final pressure of 4–5 MPa. Percentage loss of conductivity (PLC) was calculated as  $\text{PLC} = 100(1 - k_h/k_{h\text{max}})$ . Values of stem RWD corresponding to the pressures applied were obtained from the sapwood moisture release curves generated as described above. Vulnerability data reported here are means of curves obtained from three stem segments per species.

The water potential of terminal branches ( $\Psi_{br}$ ) of ten species was estimated with a pressure chamber from balance pressures of covered, non-transpiring leaves. Leaves were enclosed in aluminum foil and plastic bags in the afternoon prior to the day of measurements. At each sampling time between 0800 and 1500 hours, measurements were obtained from three to five leaves of each tree as described above for exposed leaves.

#### Whole-tree water flux

Sap flow was measured with variable-length heat-dissipation sensors (James et al. 2002) near the base of the trunk and in the crown of four trees at the Parque San Lorenzo site. Mass flow of sap in the trunk and branches was obtained by multiplying sap flux by sapwood cross-sectional area. Basal flow was measured with duplicate sets of probes installed on opposite sides of the trunk at heights of 1–2 m. The probes were installed at three to four depths in the sapwood depending on the trunk diameter. The cross-sectional area of sapwood corresponding to each probe was estimated according to James et al. (2002). Sap flow measured with probes installed in three branches in the upper crown of each tree was taken as a surrogate for transpiration (Goldstein et al. 1998) and expressed on a leaf area basis by dividing sap flow by the total leaf area distal to each set of probes. Crown conductance was estimated by dividing crown transpiration by the vapor pressure deficit measured at half-an-hour intervals at a weather station installed on the crane tower. Daily time courses of utilization of stored water for transpiration were estimated from lags in rates of change in crown and basal sap flow, as described by Goldstein et al. (1998). Positive values of crown minus basal sap flow indicate that water is being withdrawn from storage compartments located between the

upper branches and the base of the trunk. Negative values indicate recharge of *C*.

## Results

Logistical and technical difficulties prevented characterization of all of the functional traits in each of the 11 study species. Nevertheless, a number of significant species-independent relationships were obtained among the traits studied. Bulk leaf osmotic potential and daily minimum  $\Psi_L$  were linearly related ( $P = 0.003$ ) across species (Fig. 1). Because the slope of the linear regression was not significantly different from 1, bulk leaf turgor coinciding with minimum  $\Psi_L$  was similar across species ( $\sim 0.8$  MPa). Branch xylem pressure corresponding to 50% loss of hydraulic conductivity ( $P_{50}$ ) declined linearly ( $P = 0.001$ ) with daily minimum  $\Psi_{br}$  (Fig. 2). However, the slope of the relationship was significantly greater than 1 ( $P < 0.05$ ), indicating that the  $\Delta\Psi$  between  $P_{50}$  and  $\Psi_{br}$  increased as  $\Psi_{br}$  became more negative. The margin between  $\Psi_{br}$  and  $P_{50}$  increased from 0.4 MPa in the species with the least negative  $\Psi_{br}$  to 1.2 MPa in the species with the most negative  $\Psi_{br}$ . The intercept of the relationship was not significantly different from zero at  $\Psi_{br} = 0$ .

Representative sapwood water release curves for three co-occurring species having high, intermediate and low values of sapwood *C* are shown with their respective values of minimum  $\Psi_{br}$  in Fig. 3a–c. The slope of linear regressions fitted to the initial portions of the water release curves (dashed lines, Fig. 3a–c) comprising the operating range of

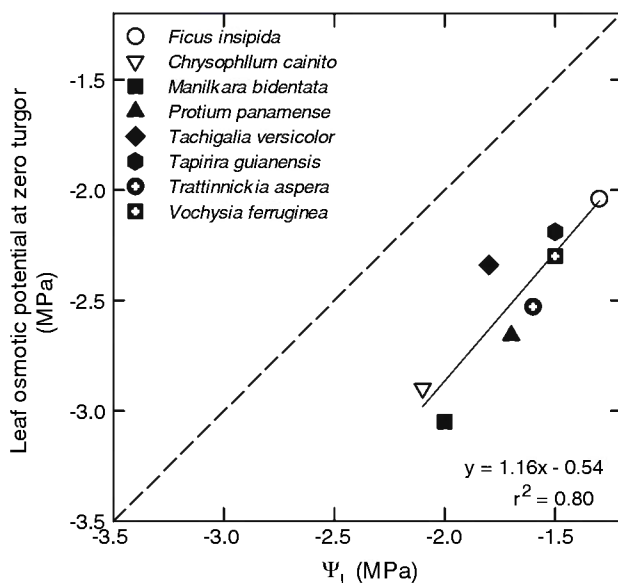


**Fig. 1** Relationship between bulk leaf osmotic potential at zero turgor and daily minimum leaf water potential ( $\Psi_L$ ) for eight tropical tree species. Dashed line indicates a 1:1 relationship

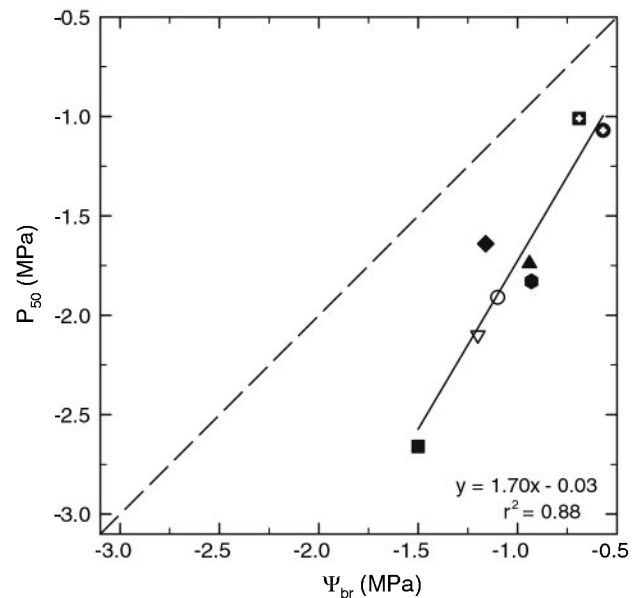


**Fig. 2** Relationship between the xylem pressure corresponding to 50% loss of conductivity ( $P_{50}$ ) in excised branch segments and minimum water potential observed in intact terminal branches ( $\Psi_{br}$ ) in the field. Symbols are as defined in Fig. 1

$\Psi_{sw}$  in vivo provided a relative measure of sapwood *C*. Minimum  $\Psi_{br}$  was never more negative than the transition region of the water release curve where  $\Psi_{sw}$  began to decline more steeply with increasing RWD (intersection of vertical and horizontal dotted lines, Fig. 3a–c). Among the ten species for which data were available, minimum  $\Psi_{br}$  ranged from  $-0.6$  to  $-1.5$  MPa, whereas the corresponding values of sapwood RWD ranged from 0.25 to 0.55 (Table 1) with a mean of  $0.39 \pm 0.03$ . The sapwood RWD at the water release curve inflection points also corresponded closely to the transition from the non-linear to linear portions of the sapwood pressure–volume curves (vertical dotted lines, Fig. 3d–f), an estimate of the bulk tissue osmotic potential at zero turgor for sapwood, which contained both non-living xylem elements and living xylem parenchyma. The relationship between sapwood turgor loss points estimated from the pressure–volume curves and minimum values of  $\Psi_{br}$  measured in the field was linear ( $P < 0.0001$ ) and not significantly different from 1:1 (Fig. 4). The  $\Psi_{sw}$  and RWD thresholds at which  $\Psi_{sw}$  began to decline more abruptly with increasing RWD also corresponded to the thresholds at which PLC began to increase more steeply with increasing branch water deficits (cf. dotted lines, Fig. 3g–i, a–c). Despite the 1.7 MPa range of  $P_{50}$  among the eight species for which data were available, the range of PLC at minimum  $\Psi_{br}$  was relatively small (Fig. 3g–i; Table 1) with a mean PLC of  $31 \pm 2\%$ .

Branch  $P_{50}$  increased linearly ( $P < 0.001$ ) with sapwood *C* (Fig. 5a) as did minimum  $\Psi_{br}$  ( $P = 0.001$ , Fig. 5b). Variation

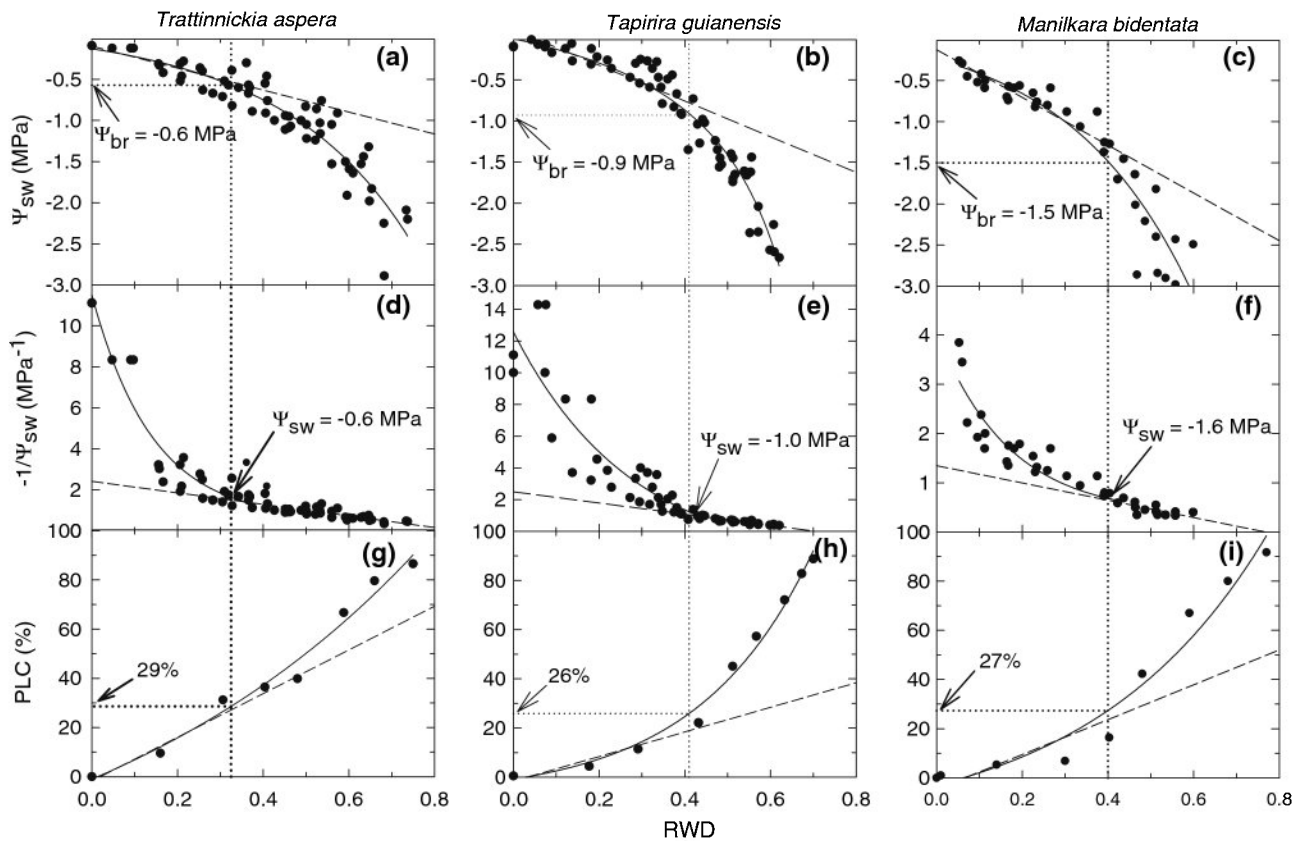


**Fig. 3** Water relations characteristics of upper branches of three co-occurring tropical forest canopy trees. **a–c** Sapwood moisture release curves showing the relationship between sapwood water potential ( $\Psi_{sw}$ ) and relative water deficit ( $RWD$ ). Vertical dotted lines indicate values of  $RWD$  corresponding to minimum values of  $\Psi_{br}$ . **d–f** Sapwood moisture release curves plotted as pressure–volume curves. Values of sapwood water potential shown correspond to the

intersection of the linear and non-linear portions of the curves ( $\Psi$  at zero turgor). **g–i** Hydraulic vulnerability curves for branches showing percent loss of conductivity ( $PLC$ ) in relation to  $RWD$ . The dashed lines are linear regressions fitted to the initial, nearly linear portions of the curves. The values of  $PLC$  shown correspond to the intersection of the fitted vulnerability curve with the vertical dotted lines ( $RWD$  at minimum  $\Psi_{br}$  measured in the field)

in  $P_{50}$  and  $\Psi_{br}$  with sapwood  $C$  was such that the difference between  $\Psi_{br}$  and  $P_{50}$ , an estimate of the safety margin for avoiding runaway embolism, decreased ( $P = 0.02$ ) with increasing sapwood  $C$  (Fig. 5c). No significant relationships between  $P_{50}$  and branch  $k_s$  ( $r^2 = 0.03$ ;  $P = 0.66$ ) or wood density ( $r^2 = 0.07$ ;  $P = 0.53$ ) were observed (data not shown).

Daily trajectories of branch transpiration and crown conductance at the mature forest site were closely associated with daily time courses of withdrawal and recharge of stored water as estimated from the difference between crown and basal sap flow (Fig. 6). All three variables increased rapidly after sunrise, but when rates of withdrawal of stored water peaked and began to decline, crown conductance also peaked and began to decline, which resulted in branch transpiration remaining nearly constant, regardless of increasing atmospheric vapor pressure deficit. Further fluctuations in withdrawal or recharge of stored water were often mirrored by corresponding fluctuations in crown conductance and branch transpiration.

## Discussion

### Coordination of leaf and stem water relations

We observed a high degree of convergence in coordination of functional traits governing leaf and stem water relations among individuals of 11 lowland tropical forest tree species. Stomatal regulation of  $\Psi_L$  was associated with minimum values of  $\Psi_{br}$  whose functional significance was similar across species. For example, minimum  $\Psi_{br}$  was associated with a relatively small range of sapwood  $RWD$  and  $PLC$  among species (Table 1). Additionally, minimum values of  $\Psi_{br}$  corresponded to bulk sapwood tissue osmotic potential at zero turgor derived from pressure–volume curves. Sapwood contains living parenchyma tissue as well as dead xylem conduits and fibers. Surveys of diffuse-porous angiosperms have shown that living axial and ray parenchyma tissue often constitute up to 40% or more of the total sapwood volume (Panshin and de Zeeuw 1980). In some tropical trees with low wood density and high water

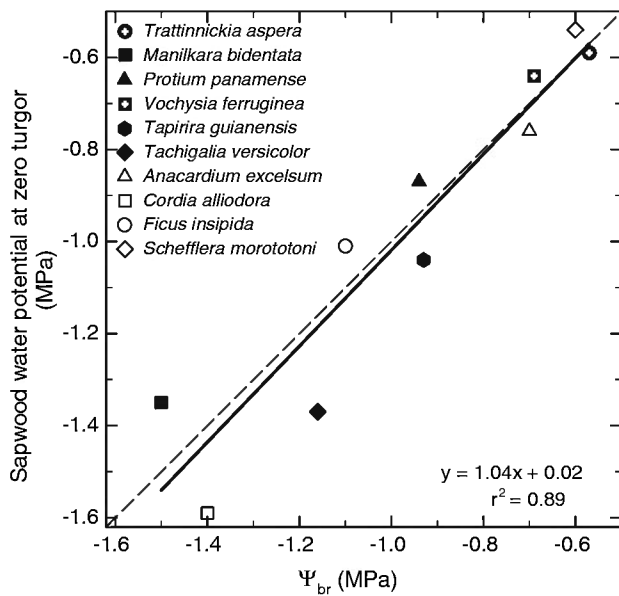


**Fig. 4**  $\Psi_{sw}$  at zero turgor in relation to minimum  $\Psi_{br}$  for ten tropical tree species. The dashed line represents a 1:1 relationship. For abbreviations, see Figs. 2 and 3

storage capacity, xylem parenchyma can occupy >75% of the total sapwood volume (Chapotin et al. 2006). Thus, sapwood pressure–volume curves should reflect the volume-weighted average of the water retention characteristics of both living and dead cells. Although we did not directly determine volume fractions of living and dead tissue in the sapwood of the species studied here, it is likely that sapwood pressure–volume curves largely reflected the osmotic characteristics of living tissue over the physiological operating ranges of  $\Psi_{sw}$  observed. Measurements of mean vessel diameter and frequency in branch sapwood of three species at each site indicated that vessel lumen area constituted only about 9% of the total cross-sectional area (K. A. McCulloh, unpublished data). Calculations based on these data, sapwood moisture release curves, minimum values of  $\Psi_{br}$  and xylem vulnerability curves suggested that water released via cavitation of vessels accounted for only about 15% of total daily reliance on *C*. The remaining 85% of daily capacitive discharge was apparently derived from parenchyma, fibers and intercellular spaces, but the relative contribution of each of these compartments was not determined.

Two of the species studied here, *Cordia alliodora* and *Schefflera morototoni*, as well as other tropical tree species have been reported to undergo diurnal depressions in leaf hydraulic conductance (Bucci et al. 2003; Brodrribb and Holbrook 2004; Meinzer et al. 2004). There is mounting evidence that rapidly reversible diurnal changes in leaf hydraulic conductance ( $K_{leaf}$ ) may constitute part of an essential hydraulic signal that enables stomata to maintain stem and leaf  $\Psi$  at set points that insure the integrity of the

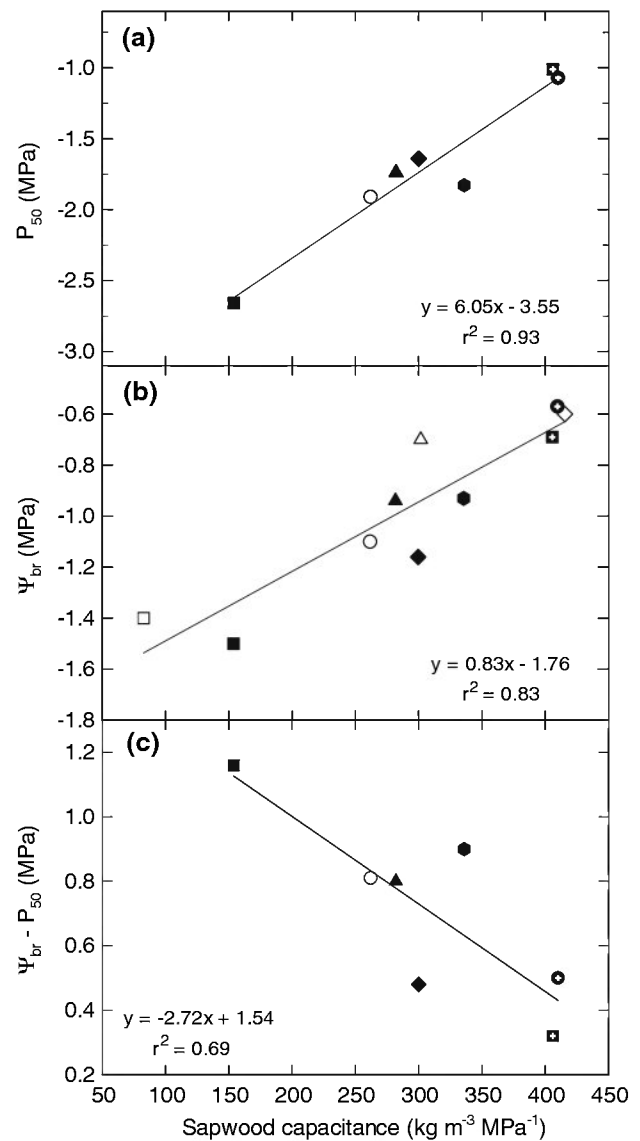


**Fig. 5** a  $P_{50}$  in excised branch segments, b minimum  $\Psi_{br}$  in the field, and c  $\Psi_{br} - P_{50}$  in relation to branch sapwood capacitance (*C*). Symbols are as defined in Fig. 1. Sapwood *C* data were not taken for one of the species in which  $P_{50}$  was determined. For abbreviations, see Fig. 2

water transport pathway upstream (Brodrribb and Holbrook 2003; Woodruff et al. 2007). Failure of stomata to respond quickly to rapid increases in transpiration could result in sharp increases in stem xylem tension and loss of conductivity, especially if water from sapwood storage has already been exhausted. Indeed, stomatal coordination of minimum leaf and stem  $\Psi$  among the species studied here resulted in minimum values of  $\Psi_{br}$  that coincided with the transition from a linear to exponential increase in embolism with increasing sapwood water deficits (Fig. 3). Consistent with this, Brodrribb et al. (2003) reported a strong correlation between  $\Psi_L$  at 50% stomatal closure and  $\Psi$  corresponding to 20% loss of stem conductivity.

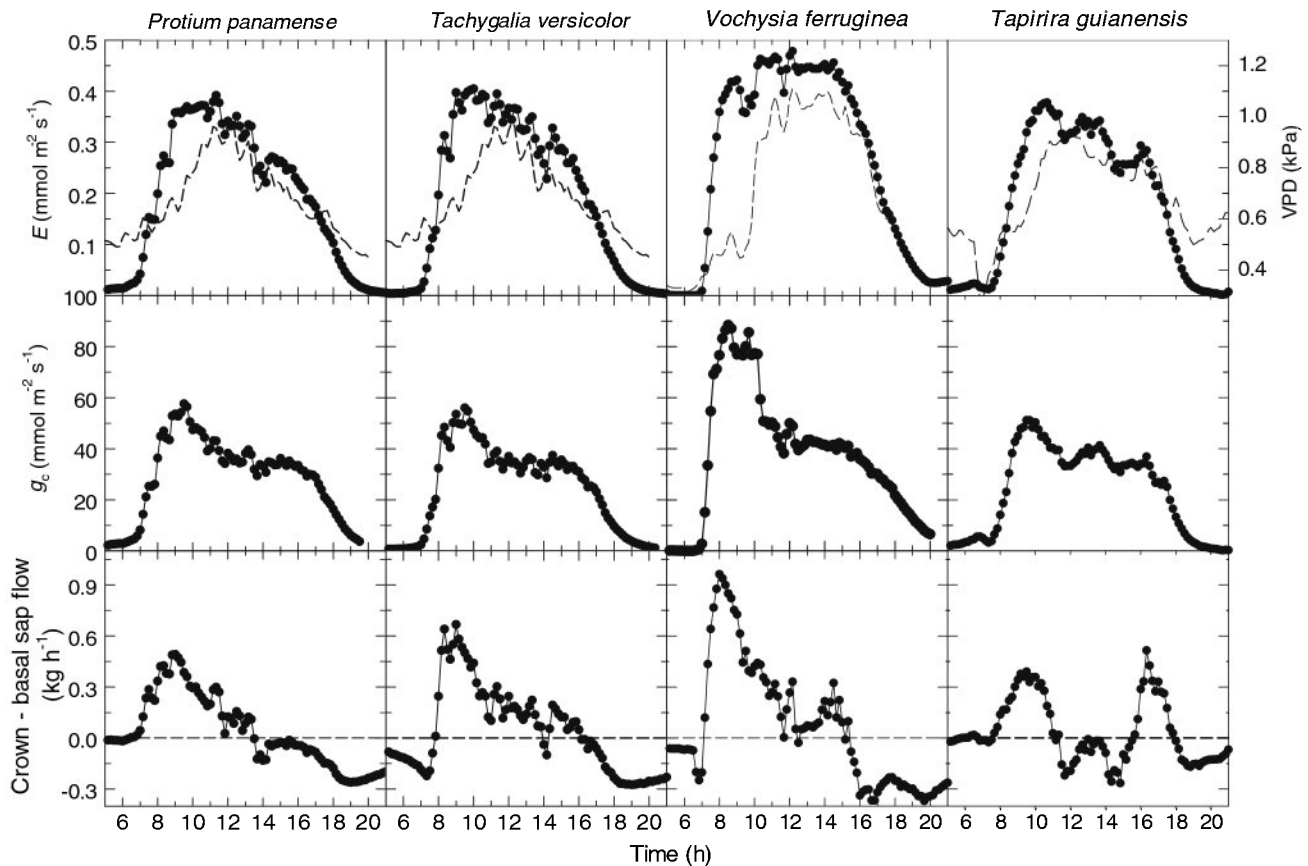


**Fig. 6** Daily courses of upper crown transpiration ( $E$ ), vapor pressure deficit ( $VPD$ ), crown conductance ( $g_c$ ) and the difference between crown and basal sap flow, a measure of discharge and recharge of  $C$ , in

four co-occurring tropical tree species. Measurement dates were 23 February 2004 for *P. panamense* and *Tachygalia versicolor*, 25 February 2004 for *V. ferruginea*, and 21 March 2004 for *Tapirira guianensis*

Although minimum values of  $\Psi_L$  showed considerable variation across species, daily minimum values of bulk leaf turgor were similar at about 0.8 MPa (Fig. 1). The extent to which this pattern reflected similar changes in leaf hydraulics was not determined. Generation of a hydraulic signal via changes in  $K_{leaf}$  does not exclude the possibility that declining turgor or volume in sapwood parenchyma cells stimulated the release of a chemical signal into the transpiration stream that ultimately influenced stomatal behavior downstream. Moreover, loss of up to 30% of sapwood conductivity upstream could contribute to an overall hydraulic signal that affected stomatal aperture. Regardless of the mechanisms involved in coordination of leaf and stem water transport properties, the behavior observed seemed to optimize capacitive discharge of water from stem tissue, while at the same time avoiding undue risk of runaway embolism.

#### Role of $C$

Although stored water typically contributes <30% to total daily transpiration even in large trees (Phillips et al. 2003; Meinzer et al. 2004), hydraulic  $C$  can have a profound

buffering effect on daily fluctuations in  $\Psi$  in leaves and terminal branches (Meinzer et al. 2003; Scholz et al. 2007). Application of an electric circuit analogy to the cohesion-tension theory indicates that even though  $C$  does not delay the onset of changes in  $\Psi$  induced by changes in water flux, it can substantially alter time constants for changes in  $\Psi$  downstream from the sources of  $C$  (Phillips et al. 2004). In *Tapirira guianensis*, for example, setting relative values of sapwood hydraulic resistance ( $R$ ) and  $C$  at 1.0 when  $\Psi_{br} = \text{zero}$  causes the relative time constant ( $\tau = R \times C$ ) to fall to about 0.25 when  $\Psi_{br} = P_{50}$  largely because of the sharp reduction in  $C$ . Thus, at  $P_{50}$  further transpiration-induced declines in  $\Psi_{br}$ , and therefore loss of conductivity, would occur about 4 times faster than in a fully hydrated branch. In all of the species studied, time constants for transpiration-induced changes in  $\Psi_{br}$  steadily diminished as  $\Psi_{br}$  declined because the relative decline in  $C$  outweighed the increase in  $R$  as sapwood water deficit increased (data not shown). The species-specific set points for  $\Psi_{br}$  appeared to represent a compromise that optimizes reliance on stored water over the range where  $C$  is nearly constant as  $\Psi_{br}$  declines, but minimizes the risk of runaway embolism as both  $C$  and its buffering effect diminish

beyond this point (Fig. 3). The strong positive relationship between xylem vulnerability and sapwood  $C$  (Fig. 5a) and the linear decline in the hydraulic safety margin ( $\Psi_{br} - P_{50}$ ) with increasing species-specific values of  $C$  (Fig. 5c) implied a trade-off between maximizing water transport and minimizing the risk of xylem embolism, and suggest a prominent role for the buffering effect of  $C$  in preserving the integrity of long-distance water transport in the species studied. Consistent with this, Pratt et al. (2007) reported that xylem vulnerability was positively related, and implosion resistance negatively related, to stem  $C$  among nine chaparral shrub species. Given the inverse relationships between xylem density and water storage capacity (Stratton et al. 2000; Bucci et al. 2004b) and between xylem density and vulnerability to embolism (Hacke et al. 2001; Pratt et al. 2007), our results further imply that fast-growing tropical early successional tree species with low wood density should possess a suite of water relations traits that include higher sapwood  $C$ , greater xylem vulnerability, and smaller diurnal fluctuations in  $\Psi_L$  than slower growing mature forest species with denser wood. However, despite a tendency for wood density to be greater among the species at the mature forest site (unpublished observations), the range of sapwood  $C$  was similar for species at both the secondary and mature forest sites (Fig. 5b) because species at the wetter mature forest site had greater values of  $C$  at a given wood density (data not shown). Generalizations about relationships between functional traits and tree successional status should thus be made with caution.

Stomatal regulation of  $\Psi_L$  in the species studied was tightly coordinated with both the intrinsic buffering capacity of the sapwood tissue upstream and critical values of sapwood water deficit corresponding to transition between a linear and exponential loss of conductivity with increasing water deficit. This conservative stomatal behavior implies that embolism in terminal branches may not be readily reversible on a daily basis. Our results further imply that terminal branches routinely lose 25–40% of their maximum conductivity (Table 1). In an earlier study conducted on 20 canopy tree species growing at the same two sites (Santiago et al. 2004) it was found that the mean native PLC of upper canopy branches was  $36 \pm 6\%$ , which is consistent with the mean of 31% for the species listed in Table 1. These findings strongly suggest that despite stomatal regulation of stem water potential to prevent runaway embolism, terminal branches of trees at both sites normally operate at about 30% below their maximum hydraulic capacity at least under midday conditions during the dry season when the measurements in the present study and that of Santiago et al. (2004) were carried out. It was not determined whether partial or complete recovery of branch conductivity occurs overnight.

## Daily dynamics of whole-tree transpiration

There was notable similarity in stomatal regulation of whole-tree transpiration among species at the Parque San Lorenzo site (Fig. 6), despite differences in tree size and functional traits such as sapwood  $C$ , branch xylem vulnerability and operating ranges of leaf and branch  $\Psi$ . Daily courses of crown conductance indicated that stomata generally began to close rapidly after attaining their maximum aperture by 0900 hours. Early stomatal restriction of transpiration occurred even though the vapor pressure deficit was around 0.5 kPa or less and soil water availability was relatively high as indicated by predawn  $\Psi_L$  of about  $-0.09$  MPa when corrected to ground level. Other studies of diurnal stomatal behavior in trees often report initiation of closing responses before 0900 hours under soil and atmospheric conditions that seem favorable for sustained stomatal opening (Roberts et al. 1990; Dye and Olbrich 1993; Loustau et al. 1996; Meinzer et al. 1999; Woodruff et al. 2007). This early to mid-morning stomatal closure has been attributed to hydraulic constraints (Meinzer et al. 1999; McDowell et al. 2005), but their specific nature is not clear. Our results show a tight synchrony between the time at which both withdrawal of stored water and crown conductance peaked and began to decline. This pattern suggests that discharge and recharge of internal  $C$  may constitute a hydraulic signal that generates variations in apparent leaf-specific conductance to which stomata respond dynamically through variation in  $\Psi_L$  (Meinzer 2002). Consistent with this, Andrade et al. (1998) observed a common positive relationship between the apparent leaf-specific conductance of the soil-to-leaf pathway and the difference between crown and basal sap flow (a measure of capacitive discharge or recharge) among five co-occurring tropical forest tree species. Apparently, the high phylogenetic and architectural diversity of tropical trees belie suites of offsetting functional traits that contribute to spatial uniformity of transpiration and other processes at the canopy level.

**Acknowledgments** This research was supported by National Science Foundation grant IBN 99-05012 to F. Meinzer and G. Goldstein. The authors thank the Smithsonian Tropical Research Institute for providing facilities and logistical support, and the expertise of the canopy crane operators. The authors are grateful to Kate McCulloh for providing data on xylem vessel diameter and frequency. This research complied with the laws of the Republic of Panama.

## References

- Andrade JL, Meinzer FC, Goldstein G, Holbrook NM, Cavellier J, Jackson P, Silvera K (1998) Regulation of water flux through trunks, branches and leaves in trees of a lowland tropical forest. *Oecologia* 115:463–471

- Begg JE, Turner NC (1970) Water potential gradients in field tobacco. *Plant Physiol* 46:343–346
- Bowman WD, Roberts SW (1985) Seasonal changes in tissue elasticity in chaparral shrubs. *Physiol Plant* 65:233–236
- Brodrribb TJ, Holbrook NM (2003) Stomatal closure during leaf dehydration, correlation with other leaf physiological traits. *Plant Physiol* 132:2166–2173
- Brodrribb TJ, Holbrook NM (2004) Diurnal depression of leaf hydraulic conductance in a tropical tree species. *Plant Cell Environ* 27:820–827
- Brodrribb TJ, Holbrook NM, Gutiérrez MV (2002) Hydraulic and photosynthetic co-ordination in seasonally dry tropical forest trees. *Plant Cell Environ* 25:1435–1444
- Brodrribb TJ, Holbrook NM, Edwards EJ, Gutiérrez MV (2003) Relations between stomatal closure, leaf turgor and xylem vulnerability in eight tropical dry forest trees. *Plant Cell Environ* 26:443–450
- Bucci SJ, Scholz FG, Goldstein G, Meinzer FC, Sternberg LDSL (2003) Dynamic changes in hydraulic conductivity in petioles of two savanna tree species: factors and mechanisms contributing to the refilling of embolized vessels. *Plant Cell Environ* 26:1633–1645
- Bucci SJ, Scholz FG, Goldstein G, Meinzer FC, Hinojosa JA, Hoffmann WA, Franco AC (2004a) Processes preventing nocturnal equilibration between leaf and soil water potential in tropical savanna woody species. *Tree Physiol* 24:1119–1127
- Bucci SJ, Goldstein G, Meinzer FC, Scholz FG, Franco AC, Bustamante M (2004b) Functional convergence in hydraulic architecture and water relations of tropical savanna trees: from leaf to whole plant. *Tree Physiol* 24:891–899
- Bucci SJ, Goldstein G, Meinzer FC, Franco AC, Campanello P, Scholz FG (2005) Mechanisms contributing to seasonal homeostasis of minimum leaf water potential and predawn disequilibrium between soil and plant water potential in Neotropical savanna trees. *Trees* 19:296–304
- Buckley TN (2005) The control of stomata by water balance. *New Phytol* 168:275–291
- Chapotin SM, Razanameharizaka JH, Nalbrook NM (2006) A biomechanical perspective on the role of large stem volume and high water content in baobab trees (*Adansonia* spp.; Bombacaceae). *Am J Bot* 93:1251–1264
- Domec J-C, Meinzer FC, Lachenbruch B, Housset J (2007) Dynamic variation in sapwood specific conductivity in six woody species. *Tree Physiol* 27:1389–1400
- Dye PJ, Olbrich BW (1993) Estimating transpiration from 6-year-old *Eucalyptus grandis* trees: development of a canopy conductance model and comparison with independent sap flux measurements. *Plant Cell Environ* 16:45–53
- Evans RD, Black RA, Link SO (1990) Rehydration-induced changes in pressure–volume relationships of *Artemisia tridentata* Nutt. ssp. *tridentata*. *Plant Cell Environ* 13:455–461
- Fisher RA, Williams M, Lobo do Vale R, Lola Da Costa A, Meir P (2006) Evidence from Amazonian forests is consistent with isohydric control of leaf water potential. *Plant Cell Environ* 29:151–165
- Franks PJ (2004) Stomatal control and hydraulic conductance, with special reference to tall trees. *Tree Physiol* 24:865–878
- Franks PJ, Drake PL, Froend RH (2007) Anisohydric but isohydrodynamic: seasonally constant plant water potential gradient explained by a stomatal control mechanism incorporating variable plant hydraulic conductance. *Plant Cell Environ* 30:19–30
- Goldstein G, Andrade JL, Meinzer FC, Holbrook NM, Cavellier J, Jackson P, Celis A (1998) Stem water storage and diurnal patterns of water use in tropical forest canopy trees. *Plant Cell Environ* 21:397–406
- Hacke UG, Sperry JS, Pockman WT, Davis SD, McCulloh KA (2001) Trends in wood density and structure are linked to prevention of xylem implosion by negative pressure. *Oecologia* 126:457–461
- Holbrook NM, Sinclair TR (1992) Water balance in the arborescent palm, *Sabal palmetto*. II. Transpiration and water storage. *Plant Cell Environ* 15:401–409
- James SA, Clearwater MJ, Meinzer FC, Goldstein G (2002) Variable length heat dissipation sensors for the measurement of sap flow in trees with deep sapwood. *Tree Physiol* 22:277–283
- Kobayashi Y, Tanaka T (2001) Water flow, hydraulic characteristics of Japanese red pine and oak trees. *Hydrol Proc* 15:1731–1750
- Loustau D, Berbigier P, Roumagnac P, Arruda-Pacheco C, David JS, Ferreira MI, Pereira JS, Tavares R (1996) Transpiration of a 64-year-old maritime pine stand in Portugal. 1. Seasonal course of water flux through maritime pine. *Oecologia* 107:33–42
- McDowell NG, Licata J, Bond BJ (2005) Environmental sensitivity of gas exchange in different-sized trees. *Oecologia* 145:9–20
- Meinzer FC (2002) Co-ordination of liquid and vapor phase water transport properties in plants. *Plant Cell Environ* 25:265–274
- Meinzer FC (2003) Functional convergence in plant responses to the environment. *Oecologia* 134:1–11
- Meinzer FC, Rundel PW, Sharifi MR, Nilsen ET (1986) Turgor and osmotic relations of the desert shrub *Larrea tridentata*. *Plant Cell Environ* 9:467–475
- Meinzer FC, Goldstein G, Jackson PJ, Holbrook NM, Gutierrez MV (1995) Environmental and physiological regulation of transpiration in tropical forest gap species: the influence of boundary layer and hydraulic properties. *Oecologia* 101:514–522
- Meinzer FC, Goldstein G, Franco AC, Bustamante M, Iglar E, Jackson P, Caldas L, Rundel PW (1999) Atmospheric and hydraulic limitations on transpiration in Brazilian cerrado woody species. *Funct Ecol* 13:273–282
- Meinzer FC, James SA, Goldstein G, Woodruff D (2003) Whole-tree water transport scales with sapwood capacitance in tropical forest canopy trees. *Plant Cell Environ* 26:1147–1155
- Meinzer FC, James SA, Goldstein G (2004) Dynamics of transpiration, sap flow and use of stored water in tropical forest canopy trees. *Tree Physiol* 24:901–909
- Meinzer FC, Brooks JR, Domec JC, Gartner BL, Warren JM, Woodruff DR, Bible K (2006) Dynamics of water transport and storage in conifers studied with deuterium and heat tracing techniques. *Plant Cell Environ* 29:105–114
- Mencuccini M (2003) The ecological significance of long-distance water transport: short-term regulation, long-term acclimation and the hydraulic costs of stature across plant life forms. *Plant Cell Environ* 26:163–182
- Panshin AJ, de Zeeuw C (1980) Textbook of wood technology. McGraw-Hill, New York
- Perämäki M, Vesala T, Nikinmaa E (2005) Modeling the dynamics of pressure propagation and diameter variation in tree sapwood. *Tree Physiol* 25:1091–1099
- Phillips NG, Ryan MG, Bond BJ, McDowell NG, Hinckley TM, Cermák J (2003) Reliance of stored water increases with tree size in three species in the Pacific Northwest. *Tree Physiol* 23:237–245
- Phillips NG, Oren R, Licata J, Linder S (2004) Time series diagnosis of tree hydraulic characteristics. *Tree Physiol* 24:879–890
- Pratt RB, Jacobsen AL, Ewers FW, Davis SD (2007) Relationships among xylem transport, biomechanics and storage in stems and roots of nine Rhamnaceae species of the California chaparral. *New Phytol* 174:787–798
- Reich PB, Walters MB, Ellsworth DS (1997) From tropics to tundra: global convergence in plant functioning. *Proc Natl Acad Sci USA* 94:13730–13734
- Roberts JM, Cabral OMR, Ferreira de Aguiar L (1990) Stomatal and boundary layer conductances in an Amazonian terra firme rain forest. *J Appl Ecol* 27:336–353
- Sack L, Holbrook NM (2006) Leaf hydraulics. *Annu Rev Plant Biol* 57:361–381

- Santiago LS, Goldstein G, Meinzer FC, Fisher JB, Machado K, Woodruff D, Jones T (2004) Leaf photosynthetic traits scale with hydraulic conductivity and wood density in Panamanian forest canopy trees. *Oecologia* 140:543–550
- Scholz FG, Bucci SJ, Goldstein G, Meinzer FC, Franco AC, Miralles-Wilhelm F (2007) Biophysical properties and functional significance of stem water storage tissues in neotropical savanna trees. *Plant Cell Environ* 30:236–248
- Sperry JS, Saliendra NZ (1994) Intra- and inter-plant variation in xylem cavitation in *Betula occidentalis*. *Plant Cell Environ* 17:1233–1241
- Stratton L, Goldstein G, Meinzer FC (2000) Stem water storage capacity and efficiency of water transport: their functional significance in a Hawaiian dry forest. *Plant Cell Environ* 23:99–106
- Tardieu F, Simonneau T (1998) Variability among species of stomatal control under fluctuating soil water status and evaporative demand: modelling isohydric and anisohydric behaviours. *J Exp Bot* 49:419–432
- Turner NC, Schulze E-D, Gollan T (1984) The response of stomata and leaf gas exchange to vapour pressure deficits and soil water content I. Species comparisons at high soil water contents. *Oecologia* 63:338–342
- Tyree MT, Hammel HT (1972) The measurement of the turgor pressure and water relations of plants by the pressure bomb technique. *J Exp Bot* 23:267–282
- Tyree MT, Sperry JS (1988) Do woody plants operate near the point of catastrophic xylem dysfunction caused by dynamic water stress? *Plant Physiol* 88:574–580
- Woodruff DR, McCulloh KA, Warren JM, Meinzer FC, Lachenbruch B (2007) Impacts of tree height on leaf hydraulic architecture and stomatal control in Douglas-fir. *Plant Cell Environ* 30:559–569
- Wright IJ, Reich PB, Westoby M, Ackerly DD, Baruch Z, Bongers F, Cavender-Bares J, Chapin T, Cornelissen JHC, Diemer M, Flexas J, Garnier E, Groom PK, Gullas J, Hikosaka K, Lamont BB, Lee T, Lusk C, Midgley J, Navas M-L, Niinemets U, Oleksyn J, Osada N, Poorter H, Poot P, Prior L, Pyankov VI, Roumet C, Thomas SC, Tjoelker MG, Veneklaas EJ, Villar R (2004) The worldwide leaf economics spectrum. *Nature* 428:821–827